Investigating the Role of Transcription Factors TWIST1, TWIST2 and PPARγ in the Progression of Nonalcoholic Steatohepatitis

Yanmei Zhang
Shandong Qianfoshan Hospital
Xiaoxiao Ge
Shandong Qianfoshan Hospital
Yongqing Li
Shandong provincial qianfoshan hospital
Sumei Lu
shandong provincial qianfoshan hospital
Wanshan Ma (mwsqianyi@163.com)
Department of laboratory medicine, Shandong provincial Qianfoshan hospital, Shandong University

Research

Keywords: Non-alcoholic fatty liver disease, hepatocyte steatosis, TWIST1, TWIST2, PPARγ

Posted Date: November 25th, 2020

DOI: https://doi.org/10.21203/rs.3.rs-112992/v1

Version of Record: A version of this preprint was published at Lipids in Health and Disease on April 20th, 2021. See the published version at https://doi.org/10.1186/s12944-021-01458-0.

Abstract

Background: To investigate the role that transcription factors TWIST1, TWIST2 and PPARγ play in nonalcoholic steatohepatitis progression.

Methods: The protein levels of TWIST1, TWIST2 and PPARγ were determined in the serum of NAFLD patients and healthy controls by ELISA. An *in vivo* model for fatty liver was established by feeding C57BL/6J mice a high fat diet (HFD). An *in vitro* model of steatosis was established by treating LO-2 cells with oleic acid (OA). RNA sequencing was performed on the untreated and OA treated LO-2 cells followed by TWIST1, TWIST2 and PPARγ gene mRNA levels analysis, Gene Ontology (GO) enrichment and pathway analysis.

Results: The TWIST2 serum protein levels decreased significantly in all fatty liver groups ($P<0.05$) while TWIST1 varied. TWIST2 tended to be lower in mice fed a HFD and was significantly lower at 3 months. Similarly, in our in vitro model, TWIST2 protein level was down significantly at 48 and 72 hours after OA treatment. RNA sequencing of the LO-2 cells showed an approximately 2.3-fold decrease in TWIST2, with TWIST1 and PPARγ no obvious change. The PPAR signaling pathway was enriched with 4 genes up regulated in OA treated cells ($P=0.0018$). IL-17 and TNF signaling pathways were enriched in OA treated cells.

Conclusions: Our results provide evidence that TWIST2 and PPARγ are important in NAFLD and shed light on a potential mechanism of steatosis.

Introduction

Non-alcoholic fatty liver disease (NAFLD) is a common chronic liver disorder characterized by lipid accumulation in hepatocytes. Currently, NAFLD affects approximately 20% – 30% of the Western population and 5% -18% of the Asian population, but is continuing to increase [1]. Moreover, being a metabolic disease, NAFLD can aggravate other metabolic syndromes, including obesity, type 2 diabetes mellitus, dyslipidaemia,hypertension and insulin resistance (IR)[2, 3]. However, the pathogenesis and molecular mechanisms of NAFLD are still unclear and further work is undoubtedly necessary.

NAFLD includes simple steatosis as well as non-alcoholic steatohepatitis (NASH), a more serious condition with associated inflammation. It is well known that NASH can progress to more serious conditions such as fibrosis, cirrhosis and hepatocellular carcinoma [4]. Most scholars have hypothesized that NASH requires two distinct processes to develop and have postulated the “two-hit theory” [5]. The basal steatosis is thought to be “the first” hit. The “second hit” is further damage to the liver caused by oxidative stress, inflammatory cytokines, endotoxins, insulin resistance and other harmful factors. Recently, the widely accepted pathogenesis of NAFLD has been updated to the “multiple hit theory”, which suggests that in the development of NAFLD many hits might work together in parallel [3, 6–8]. Obesity and IR are reported to play a fundamental role in the progression of NAFLD. High insulin levels promote lipid synthesis by increasing glycolysis in the liver [9]. In addition, high insulin also reduces the expression of ApoB-100 and microsomal triglyceride transfer protein (MTTP) leading to a reduction of VLDL output in the liver eventually leading to lipid deposition in the liver tissue [10]. IR can also cause hepatic steatosis, and it has been proposed that hepatic steatosis further aggravates hepatic insulin resistance, creating a feedback loop between the two conditions [11]. Kim, et al. suggested that hepatic steatosis could lead to IR, but some scholars believe that hepatic steatosis is not enough to cause liver IR [12, 13]. The relationship between hepatic steatosis and IR is still controversial and needs further study.

We have previously reported that two transcription factors, TWIST1 and PPARγ, have a positive regulatory role in the insulin sensitivity of 3T3-L1 adipocytes [14]. In the IR models of 3T3-L1 adipocytes and C57/BL6J mice silencing of TWIST1 expression can relieve IR to a certain degree indicating the potential clinical value of TWIST1 and PPARγ in steatosis related disease [15]. As hepatocytes are target cells of insulin, the role of TWIST1 and PPARγ in hepatocytes is undoubtedly worth further exploration. TWIST1 and PPARγ are reported to play important roles in hepatocytes. During embryonic development, TWIST plays a vital role in hepatocyte differentiation, mainly in mesoderm development, a part of the epithelial to mesenchymal transition (EMT). However, it has been shown that over expressed TWIST1 contributes to hepatocellular carcinoma (HCC) development [16]. With regard to PPARγ, while it is expressed at low levels in normal liver, it is markedly up regulated in fatty livers in animal models and in patients with NAFLD [17]. This is relevant as PPARγ promotes hepatic lipid uptake and lipid droplet formation [18].

In the present study, we will continue our previous work to explore the role and possible mechanism of TWIST1, as well as TWIST2, and PPARγ in the development of hepatocyte steatosis. Our work will mainly be based on clinical samples and in vivo and in vitro models of hepatocyte steatosis. Our results will provide evidence for role of TWIST and PPARγ in NAFLD, and clarify their function in the adipogenesis process and provide new insights into steatosis related disease.

Materials And Methods

Patient inclusion and human serum sample collection

A total of 406 individuals who had a health check-up at Shandong Provincial Qianfoshan Hospital from December 2017 to December 2018 were recruited into the present study. Following our inclusion criteria, these NAFLD patients were generally 18-60 years, with normal thyroid function, had no history of drinking, no malignancy, no viral hepatitis, no drug-induced liver disease, no autoimmune liver disease, and all other specific disease that causes fatty liver. NAFLD patients were divided into mild, moderate, and severe NAFLD groups based on abdominal ultrasound testing. Generally, the condition was diagnosed by the ultrasound physician and was dependent on the enlarged liver shape, enhanced liver echo, and the back-field attenuation. Healthy adults who were also having a health check-up at the same time had samples randomly collected. The levels of TWIST 1, TWIST 2 and PPARγ in the serum were analyzed by enzyme-linked immunosorbent assay (ELISA) per manufacturer's instructions. This study was performed in accordance with the ethical standards and was approved by the Ethics Committee of Shandong University (No: [2017] S048).

Materials and reagents

The C57/BL6 mice were purchased from the Experimental Animal Center of Shandong University. The high fat diet (HFD, No: D12492) and basal diet (No: D12450B) were both Research Diets products. The human hepatic cell line LO-2 (also named as HL-7702) was purchased from Procell Life Science& Technology Co., Ltd (Wuhan; China). The human TWIST 1, TWIST 2 and PPARγ ELISA Kits were Jianglai Biology (Shanghai, China) products. RPMI-1640 medium, fetal bovine serum (FBS) and 0.25% trypsin-0.02% EDTA were all purchased from GIBCO (Invitrogen, California, USA). The TWIST1 antibody was purchased from Sigma (St. Louis, MO, USA). TWIST2 and PPARγ antibodies were purchased from Abcam (Cambridge, MA, USA). The β-actin and the corresponding secondary antibodies, including Peroxidase-Conjugated Goat anti-Mouse IgG and Peroxidase-Conjugated Goat anti-Rabbit IgG, were purchased from ZSGB-BIO (Beijing, China). Oleic acid (OA) and all other general reagents used in this study were purchased from Sigma (St. Louis, MO, USA).

Induction of NAFLD in C57/BL6 mice

Sixty-four male C57/BL6 mice (6 weeks of age) were included in the study and housed 6 per cage. The mice were housed in a specific environment: 25°C, 55% relative humidity, cycle of 12 hours light and 12 hours dark. They were free to eat and drink tap water ad libitum. After a week they were randomly assigned to two groups, the "control group" (basal diets, 4% fat) and the "HFD group" (HFD, 60% fat). They were fed control or high fat diets for 16 weeks and the body weight was recorded every week. After the mice were euthanized, liver tissues were collected and snap frozen. H&E staining and Oil red O staining was conducted on liver sections. We carried out the additional procedures according to the 'Principles of Laboratory Animal Care' established by the National Institutes of Health. This study was performed in accordance with the ethical standards and was approved by the Ethics Committee of Shandong University (No: [2017] S048).

Introperitoneal glucose tolerance test (IPGTT) and introperitoneal insulin tolerance test (IPITT)

Before the mice were sacrificed at the 16^{th} week, IPGTT and IPITT were conducted in a portion of the mice to determine the ability of mice to respond to glucose and insulin. After fasting overnight for IPGTT or six hours for IPITT, 12 mice were injected with 50% glucose (2.0 g/kg, i.p) and 12 mice were injected with insulin (0.65 U/kg, i.p). Blood glucose levels in the mice were analyzed by means of a glucose test strip (Bayer, Germany) after blood samples were taken via the caudal vein at 0, 30, 60, 90, 120, 150 and 180 minutes after glucose and insulin injection. The area under the curve (AUC) was compared among different groups to analyze IPGTT and IPITT.

Establishment of the LO-2 hepatocyte steatosis model

The LO-2 hepatocytes were cultured in RPMI 1640 supplemented with 10% fetal bovine serum, 100 U/mL penicillin and 100 mg streptomycin. The cells were cultured in a humidified chamber at 37°C and 5% CO_2. For steatosis induction, RPMI-1640 supplemented with 10% FBS and OA (50 μg/mL) was added to the cells when they reached about 60% confluence. The culture medium and OA was replaced every 24 h for 24h, 48 h, 72h and 96h.

Hematoxylin-Eosin (H&E), Oil red O staining of frozen liver sections and LO-2 hepatocytes

After the mice were sacrificed and the livers removed and snap frozen, H&E staining was performed on frozen sections. The general steps are as follows: Methanol fixative for 60s; Hematoxylin 2 min; Washed with phosphate buffered saline (PBS) for 30s; Hydrochloric acid alcohol washed for 3s; Washed with PBS for 30s; Lithium carbonate 10s; Washed with PBS for 30s; 90% alcohol for 10s; Eosin for 5s; 90% alcohol for 5s; 95% alcohol for 20s, twice; 100% alcohol for 20s; 100% alcohol for 20s; Xylene for 30s, twice. The resulting slides were visualized with an inverted phase contrast microscope.

For Oil red O staining, LO-2 cells were grown on cover slips and after removal of cell culture medium cells were washed three times with PBS and fixed with 4% Tissue cell fixative solution (Solarbio Science) at room temperature for 10 min. Frozen slices for hepatic tissue were similarly fixed. After washing three times with PBS, the cells or frozen slices were stained with freshly diluted oil red O solution (0.1% oil red O dissolved in 60% isopropyl alcohol and 40% of distilled water) for 15-30 min. Cells or frozen slices were then washed with 60% isopropyl alcohol for 1 min and washed with PBS for three times. Images were obtained using an inverted phase contrast microscope. The oil red O staining was quantified by an absorbance assay. Briefly, the oil red O stain was solubilized with isopropyl alcohol and the optical density at 510 nm was measured by spectrophotometry (Multiskan Go, Thermo scientific). All experiments were conducted in triplicate.

Protein extraction and western blot analysis

We extracted total protein using radioimmunoprecipitation assay (RIPA) lysis buffer containing protease and phosphatase inhibitors. The protein concentration was analyzed by Pierce^{TM} BCA protein assay. The protein (40 μg for each sample) was resolved on SDS-PAGE gels, transferred to a hybond-P PVDF membrane. The membranes were blocked with 5% milk or 5% bovine serum albumin (BSA) for 1 hour. The membranes were incubated with primary antibodies (anti-TWIST1, 1:1000; anti-TWIST2, 1:1000; anti-PPARγ, 1:1000 and anti-β-actin, 1:2500) at 4°C overnight. After washing for three times (20 minutes each) with TBST, we incubated with horseradish peroxidase-conjugated anti-rabbit or anti-mouse secondary antibodies (1:5000) for 1 hour at room temperature. Blots were washed three times (20 minutes each) and we performed image development with ECL reagent. All experiments were performed in triplicate.

RNA sequencing analysis

We performed the RNA sequencing analysis using the Illumina HiSeq 4000 platform (KangChen Bio-tech, Shanghai, China). Briefly, cultured LO-2 cells were treated with DMSO (the control group) and Oleic acid (50 μg/mL, 48 h). After treatment, cells were lysed with Trizol reagent. RNA preparation and RNA sequencing was conducted by KangChen Bio-tech, Shanghai, China. Three biological replicates were prepared in each group. Genes were considered differentially expressed if the expression difference between two groups showed a two-fold change or greater ($Log_2FC>1.0$, Fold change). Gene Ontology (GO) enrichment analysis was performed and the enrichment score for Molecular Function (MF), Biological Process (BP) and Cellular Component (CC) were analyzed. Pathway-analysis for differentially expressed genes was further conducted based on Kyoto Encyclopedia of Genes and Genomes (KEGG) database.

Statistical analysis

We used the SPSS 24.0 software to analyze the data (mean ± SD). We analyzed the correlation between TWIST 1, TWIST 2, PPARγ, BMI, fasting glucose, fasting insulin, or HOMA and fatty liver severity by ANOVA. For western blots we used Image J to determine the relative gray values of each band by comparison with β-actin. We used a *t* test to compare the differences between two groups and used ANOVA to compare the differences between more than two groups. $P<0.05$ was considered as an indicator of significant difference.

Results

Analysis of TWIST1, TWIST2, and PPARγ protein levels in human serum samples

The serum samples were collected at clinical laboratory. A total of 406 human serum samples were collected in this study. The samples were divided into four groups based on abdominal ultrasound testing, with a healthy control group (n=99), mild NAFLD group (n=102), moderate NAFLD group (n=107), and a severe NAFLD group (n=98). The Materials and Methods section describes the criteria for determining whether a fatty liver is mild, moderate, or severe. The sex, age, height, and body weight were recorded for each individual, and the basic clinical characteristics of these individuals are shown in **Table 1.** They were further divided into four groups based on BMI (kg/m^2), with thin group (BMI≤18.5 kg/m^2, n=4), normal group (BMI=18.5-23.9 kg/m^2, n=84) overweight group (BMI=24-27.9 kg/m^2, n=137), and obesity group (BMI≥28 kg/m^2, n=181).

As shown in **Table 2**, fasting blood glucose and insulin levels were determined by automatic analyzer. Both the blood glucose and the blood insulin increased significantly with the severity of fatty liver disease ($P<0.05$). Spearman rank correlation analysis showed that a positive correlation was found between the severity of fatty liver disease and BMI (r=0.761, $P<0.001$) and HOMA value (r=0.607, $P<0.001$). Then, TWIST1, TWIST2 and PPARγ levels were measured in the serum of patients using ELISA kits. For TWIST1, the levels in the mild and severe fatty liver groups decreased significantly ($^{\triangle}P<0.05$, compared with healthy control), and increased significantly in the moderate fatty liver group ($^{\triangle}P<0.05$, compared with healthy control). The levels of TWIST2 in all of the fatty liver groups decreased significantly ($^{\triangle}P<0.05$, compared with healthy control). For PPARγ, compared with control group, there were no significant changes in mild fatty liver, moderate fatty liver, and severe fatty liver groups ($P>0.05$).

Characterization of the *in vivo* model of NAFLD

After 16 weeks on a high fat diet, the livers in the HFD group were enlarged and had a white hue (Fig. 1A). H&E staining (Fig. 1B) and Oil red O staining (Fig. 1C) of the livers showed increased lipid and triglyceride content in the HFD group indicative of steatosis. The mice in HFD group had a much higher body weight that increased significantly from 6 weeks of age (*P<0.05, Fig. 1D). Both IPGTT (Fig. 1E) and IPITT (Fig. 1F) of the HFD group showed decreased insulin response. TWIST1, TWIST2 and PPARγ protein levels all changed with the feeding time (Fig. 1G). While there were no significant changes in TWIST1 and PPARg (Fig. 1H, J), TWIST2 tended to be lower throughout the study and was significantly lower 3 months after the start of the HFD (Fig. 1I).

Characterization of the *in vitro* model of hepatocyte steatosis

LO-2 cells were treated with OA (50 μg/mL) for 24, 48, 72, and 96 h to induce steatosis. We could see obvious red stained lipid droplets with Oil red O staining, compared with control (Fig. 2A, B), showing that the LO-2 cell steatosis model was established.

As shown in Figure 2C, both TWIST1 and PPARγ protein expression were gradually increased with time (24, 48, 72, and 96 h) under OA treatment. However, similar increases could be found in control cells without OA exposure. The increased cell density may be the possible causes of TWSIT1 and PPARγ changes in LO-2 control cells under no external stimulation. Statistical analysis based on semi-quantity analysis under Image J software showed no significant change for TWIST1 (Fig. 2D), and PPARγ (Fig. 2F) expression between control and OA (50 μg/mL) treatment groups (P>0.05). TWIST2 was significantly reduced at 48 and 72 hours (Fig. 2E).

RNA sequencing analysis and RT-PCR both showed that TWIST2 was decreased significantly by OA treatment

RNA sequencing of the LO-2 cells treated with OA for 48 h showed that there are 1884 genes up-regulated and 1975 genes down-regulated in the OA treatment group when compared with the control group (Fig.3A). Cluster analysis for the top 20 up-regulated and down-regulated genes is shown in Fig. 3B. TWIST1 and PPARγ mRNA levels showed no significant difference (P>0.05) between the groups in our RNA sequencing results, but TWIST2 was down regulated significantly with OA treatment (P<0.05) (Fig. 3C). Further GO enrichment analysis of the RNAseq data revealed 542 differentially expressed (DE) up regulated genes and their associated biological processes (BP) (Fig.3D), and 514 DE down regulated genes and associated BP (Fig.3E).

Genes in the PPAR signaling pathway are enriched significantly based on RNA sequencing

Compared with control, the DE genes in OA (50μg/mL, 48h) treated cells are involved in 62 pathways, with 42 up regulated (top 10 shown in Figure 4 A) and 20 down regulated (top 10 shown in Figure 4B). In the top 10 up regulated pathways of DE genes, IL-17 signaling pathway [hsa04657], TNF signaling pathway [hsa04668], and PPAR signaling pathway [hsa03320] are listed. Four genes in the PPAR signaling pathway are up regulated in OA (50μg/mL, 48h) treated cells (P=0.0018). These four genes are acyl-CoA synthetase long chain family member 4 (ACSL4), angiopoietin like 4 (ANGPTL4), carnitine palmitoyltransferase 1A (CPT1A), and perilipin 4 (PLIN4). RT-PCR verified their up regulation (Fig. 4C). A schematic model for PPAR function is proposed as shown in Figure 4D. During adipogenesis, PPAR can be induced by unsaturated fatty acid or 9-cis-Retinoic-acid and could up regulate ACSL4, ANGPTL4, CPT1A, and PLIN, which can regulate lipid metabolism or adipocyte differentiation.

Discussion

In the present study, we focus on the role of TWIST1, TWIST2 and PPARγ in nonalcoholic steatohepatitis progression. To do this we examined the serum protein levels of TWIST1, TWIST2, and PPARγ in the serum of NAFLD patients with varying stages of disease and noted significant changes in the TWIST proteins. We also studied *in vitro* and *in vivo* models of the disease and noted that TWIST2 seemed to be affected the most in these models. Our results using each of these models provide additional evidence that the TWIST2 transcription factor may play a role in NAFLD.

TWIST2 seems to be particularly important in NAFLD because our results and the publication of a recent article showing that TWIST2 is involved in the development of NAFLD [19]. TWIST2 is a basic helix-loop-helix (bHLH) transcription factor that is highly related to TWIST1 and appears to have some redundant and non-redundant functions [20]. The TWIST transcription factors bind as homodimers or heterodimers to E-box consensus sites and are transcriptional activators or repressors depending on the cellular context [20, 21]. The TWIST proteins have been extensively studied for their oncogenic properties and their role in epithelial-mesenchymal transition (EMT), but their involvement in other processes is less well known [22]. The *twist2*-null mice have many abnormalities in fat and glucose metabolism and are presumed to die soon after birth because of the up regulation of cytokines in a NF-κB-dependent manner [23]. We saw a decrease of

TWIST 2 protein in our *in vitro* and *in vivo* models of NAFLD. Interestingly, we also noticed a decrease in TWIST2 protein levels in the serum of NAFLD patients at all stages of the disease. This suggests that in NAFLD reduction of the TWIST2 protein may be an early event that increases inflammation. It also suggests that TWIST2 protein levels in serum may be a biomarker of NAFLD. It has recently been shown that TWIST1 mRNA and protein can be found in the exosomes secreted from hepatic stellate cells (HSCs) and that the levels of TWIST1 mRNA and protein decrease in models of hepatic injury and fibrosis [24]. It is likely that TWIST2 is also being secreted from the liver compartment and that changes in TWIST2 protein content can be indicative of a developing disease process.

TWIST1 serum protein levels varied greatly with severity of disease with significantly lower levels in the mild fatty liver group and significantly higher levels in the moderate fatty liver group. The level of TWIST1 protein in the severe fatty liver group was the same as the control group. This pattern of TWIST1 serum protein may indicate complex regulation of the TWIST1 gene during development of NAFLD. TWIST1 is considered an anti-inflammatory marker as low mRNA and protein expression of TWIST1 is associated with increased expression of proinflammatory cytokines and decreased insulin sensitivity in humans [25]. Lower levels of TWIST1 in early stages of NAFLD may lead to increased inflammation and disease progression.

Increased protein expression of PPAR is a general property of steatotic livers. The contribution of PPAR is to the maintenance of a steatotic phenotype in liver cells [26]. PPARγ is capable of activating the expression of genes involved in TG accumulation in hepatocytes and promoting the generation of fatty liver [27]. While we did not see any changes in PPAR*γ* protein levels in the patient serum, or in our *in vivo* and *in vitro* models, our RNA sequence analysis of OA treated cells suggested that the PPAR signaling pathway was involved in the hepatic steatosis process. We believe that the PPARγ transcription factor may regulate downstream lipid metabolism or adipocyte differentiation through ACSL4, ANGPTL4, CPT1A, and PLIN4. Further investigation into the mechanism of how PPARγ contributes to NAFLD is warranted.

Chronic inflammation has also been implicated in the development and progression of NAFLD [28, 29]. TWIST1 and TWIST2 have been shown to reduce inflammation by inhibition of the NF-kB pathway [21, 23]. As already mentioned, twist-2 deficient mice produce high levels of cytokines [23]. An interesting finding of the GO analysis of the RNA sequencing data revealed an enhanced IL-17 signaling pathway in OA treated cells. IL-17 signaling has become of greater significance in NAFLD in recent years [30]. We also saw an enhancement in the TNF signaling pathway, another important inflammatory pathway implicated in NAFLD [31–33].

There are some limitations in this study. Although we suggested a pathway for the action of PPARγ, but the mechanism of how PPARγ contributes to NAFLD is unclear. To test PPARγ pathway with inhibitors or knockdown is necessary. About TWIST2, the related mechanism is also important to study in validating TWIST2 as a biomarker.

With the increasing incidence of NAFLD around the world, it is becoming increasingly clear that more research into mechanisms of this disease and a method of early detection will be needed.

Conclusions

In summary, we present data that TWIST2 and PPARγ are important in NAFLD and shed light on a potential mechanism of steatosis. We show that a simple blood test for TWIST2, a potential biomarker, may allow one to detect the early stages of NAFLD. Future studies will be necessary to clarify the roles of these genes and their pathways in NAFLD and validate TWIST2 as a biomarker.

Declarations

-Ethics approval and consent to participate

This study was performed in accordance with the ethical standards and was approved by the Ethics Committee of Shandong University (No: [2017] S048). Informed consent was obtained from all individual participants included in the study.

-Consent for publication

Not applicable.

-Availability of data and materials

The data will be available on request.

-Competing interests

The authors declare that they have no conflict of interest.

-Funding

This study was funded by the Key Technology Research and Development Program of Shandong (No. 2017G006024); National Natural Science Foundation of China (No. 81400843); Natural Science Foundation of Shandong Province (No. ZR2014HP033); Cultivation Fund of National Natural Science Foundation of China in Shandong Provincial Qianfoshan hospital (No. QYPY2020NSFC1004).

-Authors' contributions

SML and WSM contributed to funding acquisition, study concept, study design, data interpretation and revision of manuscript. YMZ and XXG performed most of the experiments, and contributed to data collection, data analysis and original draft writing; YQL, MJH, and YYZ contributed to data analysis; BYZ, PG, and TS performed some part of the research. All authors read and approved the final manuscript.

-Acknowledgements

RNA sequencing analysis were performed by KangChen Bio-tech, Shanghai, China

-Author details

[1]Department of Laboratory Medicine, Shandong Provincial Qianfoshan Hospital, Shandong University, Jinan, Shandong 250014, P. R.China. [2]Department of Laboratory Medicine, The First Affiliated Hospital of Shandong First Medical University, Jinan, Shandong 250014, P. R. China. [3]Medical Research Center, The First Affiliated Hospital of Shandong First Medical University, Jinan, Shandong 250014, P. R. China. [4]Department of Clinical Laboratory, the Affiliated Hospital of Shandong University of Traditional Chinese Medicine, Jinan 250014, Shandong, China.

References

1. Povero D, Feldstein AE. Novel Molecular Mechanisms in the Development of Non-Alcoholic Steatohepatitis. Diabetes Metab J. 2016;40:1–11.
2. Bellentani S. The epidemiology of non-alcoholic fatty liver disease. Liver Int. 2017;37(Suppl 1):81–4.
3. Watanabe S, Hashimoto E, Ikejima K, Uto H, Ono M, Sumida Y, Seike M, Takei Y, Takehara T, Tokushige K, et al. Evidence-based clinical practice guidelines for nonalcoholic fatty liver disease/nonalcoholic steatohepatitis. Hepatol Res. 2015;45:363–77.
4. Bashiri A, Nesan D, Tavallaee G, Sue-Chue-Lam I, Chien K, Maguire GF, Naples M, Zhang J, Magomedova L, Adeli K, et al. Cellular cholesterol accumulation modulates high fat high sucrose (HFHS) diet-induced ER stress and hepatic inflammasome activation in the development of non-alcoholic steatohepatitis. Biochim Biophys Acta. 2016;1861:594–605.
5. Day CP, James OF. Steatohepatitis: a tale of two "hits". Gastroenterology. 1998;114:842–5.
6. Tilg H, Moschen AR. Evolution of inflammation in nonalcoholic fatty liver disease: the multiple parallel hits hypothesis. Hepatology. 2010;52:1836–46.
7. Takaki A, Kawai D, Yamamoto K. Molecular mechanisms and new treatment strategies for non-alcoholic steatohepatitis (NASH). Int J Mol Sci. 2014;15:7352–79.
8. Okubo H, Kushiyama A, Sakoda H, Nakatsu Y, Iizuka M, Taki N, Fujishiro M, Fukushima T, Kamata H, Nagamachi A, et al. Involvement of resistin-like molecule beta in the development of methionine-choline deficient diet-induced non-alcoholic steatohepatitis in mice. Sci Rep. 2016;6:20157.
9. Petta S, Muratore C, Craxi A. Non-alcoholic fatty liver disease pathogenesis: the present and the future. Dig Liver Dis. 2009;41:615–25.
10. Gruben N, Shiri-Sverdlov R, Koonen DP, Hofker MH. Nonalcoholic fatty liver disease: A main driver of insulin resistance or a dangerous liaison? Biochim Biophys Acta. 2014;1842:2329–43.
11. Hebbard L, George J. Animal models of nonalcoholic fatty liver disease. Nat Rev Gastroenterol Hepatol. 2011;8:35–44.
12. Kim JY, Lee C, Oh M, Im JA, Lee JW, Chu SH, Lee H, Jeon JY. Relationship between non-alcoholic fatty liver disease, metabolic syndrome and insulin resistance in Korean adults: A cross-sectional study. Clin Chim Acta. 2016;458:12–7.
13. Colombo M, Raposo G, Thery C. Biogenesis, secretion, and intercellular interactions of exosomes and other extracellular vesicles. Annu Rev Cell Dev Biol. 2014;30:255–89.
14. Ren R, Chen Z, Zhao X, Sun T, Zhang Y, Chen J, Lu S, Ma W. A possible regulatory link between Twist 1 and PPARgamma gene regulation in 3T3-L1 adipocytes. Lipids Health Dis. 2016;15:189.

15. Lu S, Wang H, Ren R, Shi X, Zhang Y, Ma W. Reduced expression of Twist 1 is protective against insulin resistance of adipocytes and involves mitochondrial dysfunction. Sci Rep. 2018;8:12590.
16. Zou H, Feng X, Cao JG. Twist in hepatocellular carcinoma: pathophysiology and therapeutics. Hepatol Int. 2015;9:399–405.
17. Matsusue K, Haluzik M, Lambert G, Yim SH, Gavrilova O, Ward JM, Brewer B Jr, Reitman ML, Gonzalez FJ. Liver-specific disruption of PPARgamma in leptin-deficient mice improves fatty liver but aggravates diabetic phenotypes. J Clin Invest. 2003;111:737–47.
18. Zhang W, Sun Q, Zhong W, Sun X, Zhou Z. Hepatic Peroxisome Proliferator-Activated Receptor Gamma Signaling Contributes to Alcohol-Induced Hepatic Steatosis and Inflammation in Mice. Alcohol Clin Exp Res. 2016;40:988–99.
19. Zhou L, Li Q, Chen A, Liu N, Chen N, Chen X, Zhu L, Xia B, Gong Y, Chen X. KLF15-activating Twist2 ameliorated hepatic steatosis by inhibiting inflammation and improving mitochondrial dysfunction via NF-kappaB-FGF21 or SREBP1c-FGF21 pathway. FASEB J. 2019;33:14254–69.
20. Franco HL, Casasnovas J, Rodriguez-Medina JR, Cadilla CL. Redundant or separate entities?–roles of Twist1 and Twist2 as molecular switches during gene transcription. Nucleic Acids Res. 2011;39:1177–86.
21. Merindol N, Riquet A, Szablewski V, Eliaou JF, Puisieux A, Bonnefoy N. The emerging role of Twist proteins in hematopoietic cells and hematological malignancies. Blood Cancer J. 2014;4:e206.
22. Ansieau S, Bastid J, Doreau A, Morel AP, Bouchet BP, Thomas C, Fauvet F, Puisieux I, Doglioni C, Piccinin S, et al. Induction of EMT by twist proteins as a collateral effect of tumor-promoting inactivation of premature senescence. Cancer Cell. 2008;14:79–89.
23. Sosic D, Richardson JA, Yu K, Ornitz DM, Olson EN. Twist regulates cytokine gene expression through a negative feedback loop that represses NF-kappaB activity. Cell. 2003;112:169–80.
24. Chen L, Chen R, Kemper S, Charrier A, Brigstock DR. Suppression of fibrogenic signaling in hepatic stellate cells by Twist1-dependent microRNA-214 expression: Role of exosomes in horizontal transfer of Twist1. Am J Physiol Gastrointest Liver Physiol. 2015;309:G491–9.
25. Lallukka S, Sevastianova K, Perttila J, Hakkarainen A, Orho-Melander M, Lundbom N, Olkkonen VM, Yki-Jarvinen H. Adipose tissue is inflamed in NAFLD due to obesity but not in NAFLD due to genetic variation in PNPLA3. Diabetologia. 2013;56:886–92.
26. Moran-Salvador E, Lopez-Parra M, Garcia-Alonso V, Titos E, Martinez-Clemente M, Gonzalez-Periz A, Lopez-Vicario C, Barak Y, Arroyo V, Claria J. Role for PPARgamma in obesity-induced hepatic steatosis as determined by hepatocyte- and macrophage-specific conditional knockouts. FASEB J. 2011;25:2538–50.
27. Gavrilova O, Haluzik M, Matsusue K, Cutson JJ, Johnson L, Dietz KR, Nicol CJ, Vinson C, Gonzalez FJ, Reitman ML. Liver peroxisome proliferator-activated receptor gamma contributes to hepatic steatosis, triglyceride clearance, and regulation of body fat mass. J Biol Chem. 2003;278:34268–76.
28. Farrell GC, van Rooyen D, Gan L, Chitturi S. NASH is an Inflammatory Disorder: Pathogenic, Prognostic and Therapeutic Implications. Gut Liver. 2012;6:149–71.
29. Del Campo JA, Gallego P, Grande L. Role of inflammatory response in liver diseases: Therapeutic strategies. World J Hepatol. 2018;10:1–7.
30. Beringer A, Miossec P. IL-17 and IL-17-producing cells and liver diseases, with focus on autoimmune liver diseases. Autoimmun Rev. 2018;17:1176–85.
31. Braunersreuther V, Viviani GL, Mach F, Montecucco F. Role of cytokines and chemokines in non-alcoholic fatty liver disease. World J Gastroenterol. 2012;18:727–35.
32. Kakino S, Ohki T, Nakayama H, Yuan X, Otabe S, Hashinaga T, Wada N, Kurita Y, Tanaka K, Hara K, et al. Pivotal Role of TNF-alpha in the Development and Progression of Nonalcoholic Fatty Liver Disease in a Murine Model. Horm Metab Res. 2018;50:80–7.
33. Younossi ZM. Non-alcoholic fatty liver disease - A global public health perspective. J Hepatol. 2019;70:531–44.

Tables

Table 1 Basic information of human serum samples (n=406)

Parameter	Number
Sex	
male	344
female	62
Age	
18-44	301
45-59	105
BMI（Kg/m^2）	
＜18.5	4
18.5-23.9	84
24-27.9	137
≥28	181
fatty liver	
healthy control	99
mild fatty liver	102
moderate fatty liver	107
severe fatty liver	98

Table 2. Data analysis of human serum sample

parameter / groups	BMI （ $\bar{X}$±SD）	glucose (mmol/L, $\bar{X}$±SD)	insulin (mIU/L , $\bar{X}$±SD)	HOMA （ $\bar{X}$±SD）	Twist 1 concentration （pg/mL , $\bar{X}$±SD）	Twist 2 concentration （pg/mL , $\bar{X}$±SD）	PPARγ concentration （mmol/L , $\bar{X}$±SD）
healthy control	22.42±2.54$^{□,☆,※}$	4.98±0.50$^{□,☆,※}$	6.93±3.12$^{□,☆,※}$	1.54±0.74$^{□,☆,※}$	287.54±264.02$^{□,☆}$	2.63±2.26	258.88±241.26
mild fatty liver	26.32±2.45$^{△,☆,※}$	5.35±0.50$^{△,☆,※}$	9.19±4.18$^{△,☆,※}$	2.19±1.02$^{△,☆,※}$	176.62±166.08$^{△,☆,※}$	2.00±1.34$^{△}$	227.84±208.65
moderate fatty liver	28.25±2.75$^{△,□,※}$	5.92±1.59$^{△,□,※}$	11.82±6.77$^{△,□,※}$	3.15±2.07$^{△,□,※}$	380.39±331.48$^{△,□,※}$	2.04±1.37$^{△}$	216.30±177.04
severe fatty liver	31.30±3.31$^{△,□,☆}$	6.29±1.93$^{△,□,☆}$	15.29±7.66$^{△,□,☆}$	4.20±2.23$^{△,□,☆}$	279.26±238.77$^{□,☆}$	2.06±1.16$^{△}$	225.72±182.68

note: $^{△}P$＜0.05, compared with healthy control；$^{□}P$＜0.05, compared with mild fatty liver；$^{☆}P$＜0.05, compared with moderate fatty liver；$^{※}P$＜0.05, compared with severe fatty liver.

Table 3. The details of top 20 up-reguated and down-regulated genes under oleic acid treatment by RNA sequencing

Gene_Name	Trans_Name	log2FC	Fold_Change	p_value	Gene_Name	Trans_Name	log2FC	Fold_Change	p_value
Up-reguated genes					Down-reguated genes				
ASNS	ASNS-209	4.9946	31.8794	0.0000	APLP2	APLP2-201	-3.2019	0.1087	0.0001
APLP2	APLP2-202	4.0958	17.0984	0.0070	DDX27	DDX27-206	-3.1990	0.1089	0.0193
PSAP	PSAP-201	4.0106	16.1183	0.0283	CARD10	CARD10-203	-2.9708	0.1276	0.0235
EIF4G1	EIF4G1-221	3.7234	13.2089	0.0349	JADE3	JADE3-203	-2.7405	0.1496	0.0000
ANGPTL4	ANGPTL4-202	3.5879	12.0241	0.0008	APOL2	APOL2-201	-2.7045	0.1534	0.0246
NDUFS8	NDUFS8-210	3.3598	10.2658	0.0235	POLR2A	POLR2A-201	-2.5492	0.1709	0.0266
POLR2B	POLR2B-213	3.3478	10.1812	0.0213	KIF14	KIF14-202	-2.5153	0.1749	0.0272
SERPINE2	SERPINE2-203	3.3009	9.8552	0.0139	CD59	CD59-203	-2.4796	0.1793	0.0002
HAX1	HAX1-202	3.1570	8.9197	0.0238	KATNA1	KATNA1-205	-2.3728	0.1931	0.0247
CCDC47	CCDC47-207	3.1261	8.7309	0.0229	EIF4G1	EIF4G1-216	-2.3661	0.1940	0.0057
TIPARP	TIPARP-206	3.0047	8.0262	0.0214	POLR2B	POLR2B-205	-2.3462	0.1967	0.0220
ANGPTL4	ANGPTL4-201	2.9858	7.9219	0.0001	ATP5G2	ATP5G2-204	-2.3328	0.1985	0.0145
UBA2	UBA2-208	2.8114	7.0199	0.0272	NOP2	NOP2-203	-2.3103	0.2016	0.0275
EIF4G1	EIF4G1-207	2.6434	6.2481	0.0280	GPANK1	GPANK1-201	-2.2093	0.2162	0.0022
PPP2R2A	PPP2R2A-201	2.5557	5.8797	0.0221	SEC22C	SEC22C-205	-2.1893	0.2193	0.0258
PDK4	PDK4-201	2.5308	5.7790	0.0000	ALPI	ALPI-201	-2.1868	0.2196	0.0045
ZFAND2B	ZFAND2B-206	2.4906	5.6202	0.0000	CTSA	CTSA-201	-2.1791	0.2208	0.0134
DDX19B	DDX19B-208	2.4219	5.3586	0.0370	ALDH3B1	ALDH3B1-208	-2.1746	0.2215	0.0139
ZYX	ZYX-203	2.4101	5.3151	0.0480	MEOX1	MEOX1-202	-2.1356	0.2276	0.0000
WASHC5	WASHC5-202	2.2769	4.8462	0.0226	SNX3	SNX3-204	-2.1237	0.2295	0.0156

Figures

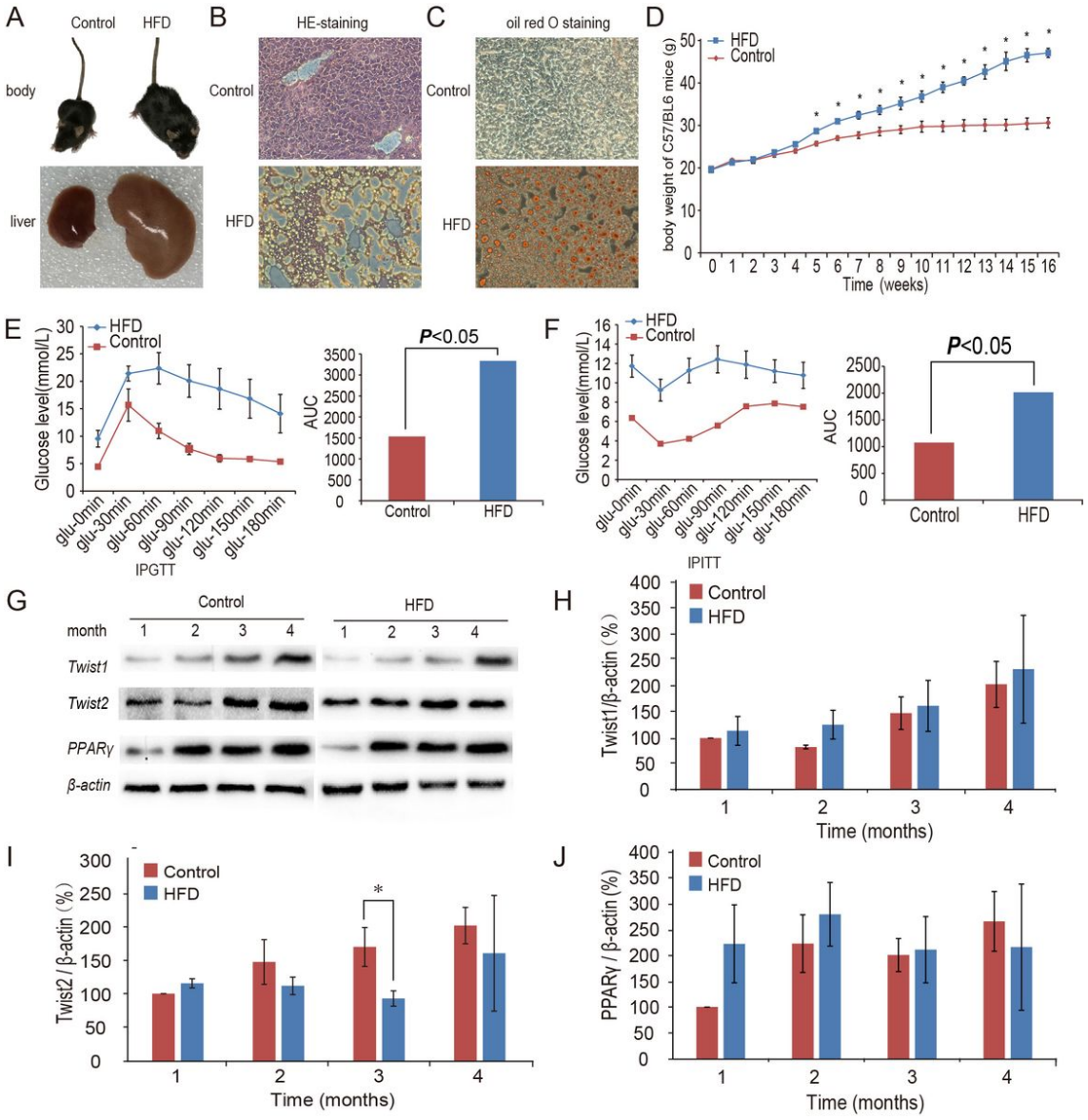

Figure 1

Characterization of in vivo model of fatty liver disease and changes in TWIST1, TWIST2 and PPARγ protein expression in liver A) Comparison of the size of control and HFD group mice and their livers. B) H&E staining of livers for control and HFD mice. C) Oil red O staining of livers from control and HFD group mice. D) Body weight changes with time. E) IPGTT detection. F) IPITT detection. G) Relative protein levels of TWIST1, TWIST2 and PPARγ. H/I/J) Semi-quantification of TWIST1 (H), TWIST2 (I), and PPARγ (J).

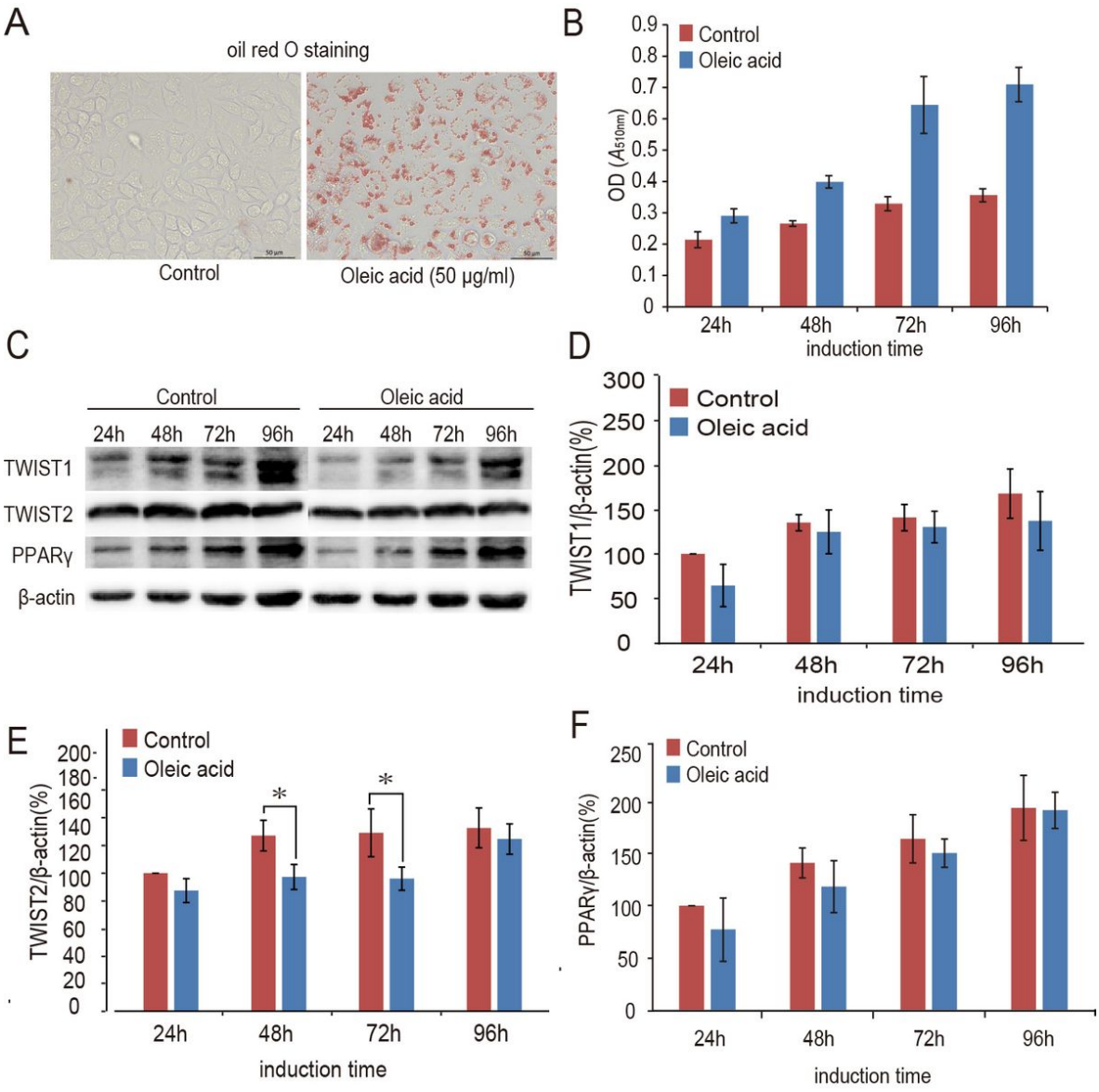

Figure 2

The LO-2 steatosis model shows increased lipid uptake but no changes in TWIST1, TWIST2, and PPARγ protein expression. A: Oil red O staining in control and oleic acid (50 μg/mL) group. B: OD value for oil red O staining in control and oleic acid group. C: TWIST 1, TWIST 2 and PPARγ expression in control and oleic acid treatment groups. β-actin was used as a loading control. D/E/F: Semi-quantification of TWIST 1 (D), TWIST 2 (E), PPARγ (F).

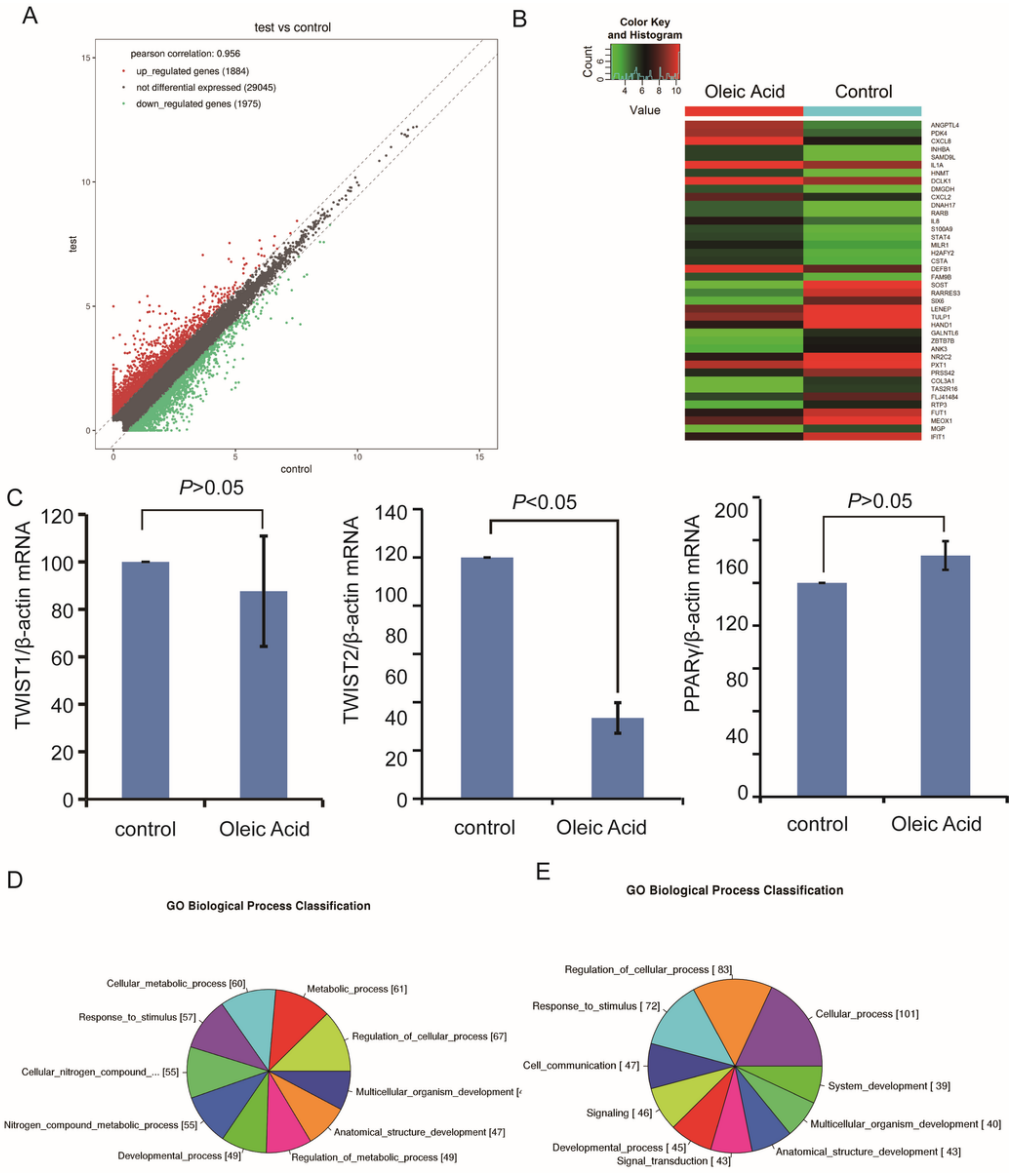

Figure 3

RNA sequencing analysis of the transcriptional changes and GO biological process analysis of LO-2 cells treated with OA (50 μg/mL, 48h). A) The mRNA scatter map of control and test group. B) Heat map of top 20 up-regulated and down-regulated genes in OA treatment (50 μg/mL, 48h) group. C) TWIST 1, TWIST 2 and PPARγ mRNA changes in OA treatment (50 μg/mL, 48h) group based on RT-PCR. D) The up-regulated genes classification for GO biological process. E) The down-regulated genes classification for GO biological process.

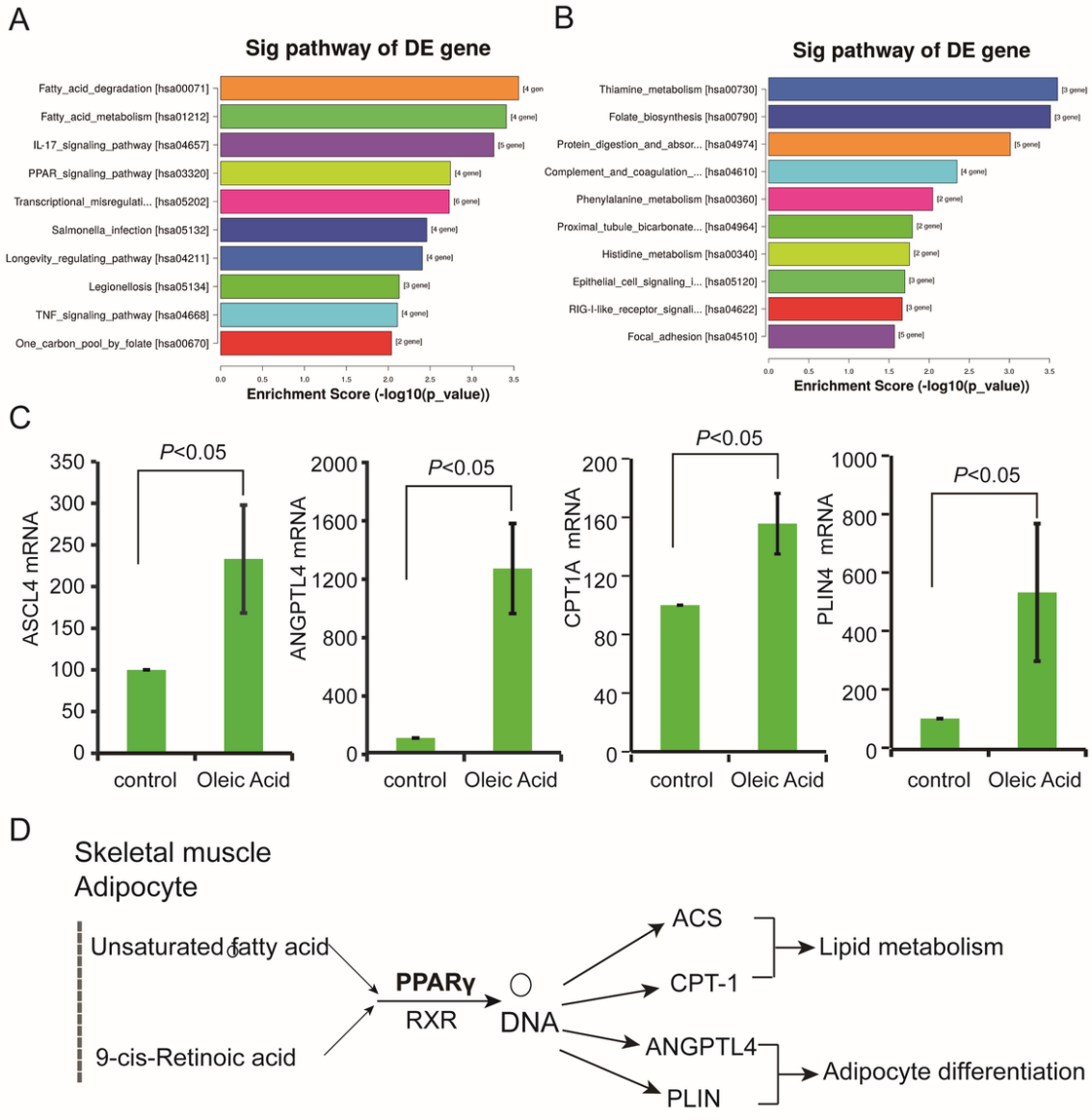

Figure 4

PPAR signaling pathway genes are enriched significantly by OA treatment. A) The top 10 up-regulated pathways of DE genes. B) The top 10 down-regulated pathways of DE genes. C) The mRNA levels of four genes of PPAR signaling pathway, including ASCL4, ANGPTL4, CPT1A, and PLIN4, based on RT-PCR. D) Schematic model of PPARγ pathway regulated genes.